

A fast and memory-efficient algorithm for smooth interpolation of polyrigid transformations: application to human joint tracking

Karim Makki^{1,2}, Bhushan Borotikar⁴, Marc Garetier⁵, Sylvain Brochard⁴, Douraied Ben Salem³, and François Rousseau¹

¹Institut Mines Télécom Atlantique, LaTIM U1101 INSERM, UBL, Brest, France.

²Aix Marseille Univ, LIS UMR 7020 CNRS, Marseille, France.

³Department of Neuroradiology, Forensic Imaging Unit, H. La Cavale Blanche, CHRU of Brest, LaTIM U1101 INSERM, Brest, France.

⁴University of Western Brittany, LaTIM U1101 INSERM, Brest, France.

⁵Department of Radiology, Military Teaching Hospital Clermont-Tonnerre, LaTIM U1101 INSERM, Brest, France.

Abstract The log Euclidean polyrigid registration framework provides a way to smoothly estimate and interpolate poly-rigid/affine transformations for which the invertibility is guaranteed. This powerful and flexible mathematical framework is currently being used to track the human joint dynamics by first imposing bone rigidity constraints in order to synthesize the spatio-temporal joint deformations later. However, since no closed-form exists, then a computationally expensive integration of ordinary differential equations (ODEs) is required to perform image registration using this framework. To tackle this problem, the exponential map for solving these ODEs is computed using the scaling and squaring method in the literature. In this paper, we propose an algorithm using a matrix diagonalization based method for smooth interpolation of homogeneous polyrigid transformations of human joints during motion. The use of this alternative computational approach to integrate ODEs is well motivated by the fact that bone rigid transformations satisfy the mechanical constraints of human joint motion, which provide conditions that guarantee the diagonalizability of local bone transformations and consequently of the resulting joint transformations. In a comparison with the scaling and squaring method, we discuss the usefulness of the matrix eigendecomposition technique which reduces significantly the computational burden associated with the computation of matrix exponential over a dense regular grid. Finally, we have applied the method to enhance the temporal resolution of dynamic MRI sequences of the ankle joint. To conclude, numerical experiments show that the eigendecomposition method is more capable of balancing the trade-off between accuracy, computation time, and memory requirements.

Keywords Diffeomorphic registration · Differential geometry · Exponential map · Lie theory · Matrix eigendecomposition · Motion interpolation · ODEs

1 Introduction

Non-rigid or deformable registration is an important tool for assessing spatial and temporal changes between images [10, 29]. It allows a non-uniform mapping between the source and target images. Among these non-rigid registration techniques are the diffeomorphic ones which have presented some interesting properties such as invertibility, differentiability, and smoothness of the resulting deformation fields. Furthermore, these techniques are suitable for parameterizing the non-linear deformations of anatomical structures or shapes which include the aspect of change over time [4, 11]. The Log Euclidean Polyrigid Framework (LEPF) is a parametric registration approach that composes a set of rigid transformations into a global diffeomorphism [4, 3]. The main idea is to parameterize a non-linear geometrical deformation with a small number of flexible degrees of freedom. Hence, it can be used to estimate human joint deformations by fusing a set of local bone rigid transformations, composing the joint of interest [20]. This approach, which is based on solving a first order *autonomous* ODE modeling the temporal evolution of a dynamical system, offers the possibility to estimate *infinitesimal diffeomorphisms*, parameterized by a dynamical time scale, via the exponential map from *Lie Algebra* to the corresponding Lie group. This framework maps the interpolation of a deformation field into the tangent space, and then transforms the resulting velocity-vector field back onto the manifold. Which makes it possible to estimate smooth deformation fields in continuous time where the *invertibility* is guaranteed. The LEPF can be used to estimate a smooth and continuous curves of moving articulated structures by interpolating the estimated polyrigid joint transformations in the domain of matrix logarithms. Which is in fact a generalization of the parameterization of rigid body transformations via the exponential map, as presented in [30, 7, 6, 28].

Since the LEPF relies on the computationally heavy solution of an ODE, the efficient computation of the exponential map over a regular grid requires the implementation of a fast algorithm to deal with the high-number of point trajectories to be estimated simultaneously. In this context, *Arsigny et al.* have proposed to use a fast algorithm employing the scaling and squaring method [3]. The major advantage of this technique is that it allows an accurate approximation of the exponential map regardless of whether the matrices are diagonalizable or not. However, this method have a high memory requirement to store all matrices in the main computer memory during the repeated squarings.

Towards the end of the 1970s, *Moler and Van Loan* have synthetized a study to present the different ways of computing the exponential of a square matrix [23]. This study has been revisited more than two decades later in [24] to take advantage of the advances of computational resources and to classify the existing methods and algorithms in terms of generality, accuracy, storage requirements, and efficiency. This study has pointed out that the algorithms which avoid use of the eigenvalues are more time-consuming for any particular problem.

Inspired by these conclusions, we propose to generate trajectories and motion interpolants from bone rigid transformations by scaling the transformation eigenvalues using a matrix-diagonalization based method.

The matrix diagonalization method has been already used to interpolate 3×3 symmetric positive-definite matrices (*i.e.* tensor matrices) in [5]. A symmetric

positive-definite A matrix has always a spectral decomposition $A = QDQ^T$, where Q is orthogonal and D is diagonal with positive diagonal elements, and then $\exp(t.\log(A)) = Q.\exp(t.\log(D)).Q^T$ $t \in \{0,1\}$ are also symmetric positive definite as they still representing infinitesimal tensors. However, this computational approach has never been used to interpolate 4×4 homogeneous transformations and the difficulty is to deal with these non symmetric matrices with nontrivial rotations generated by a linear dynamical system. In classical mechanics, one of the well known properties is that an homogeneous 4×4 transformation matrix cannot be diagonalized and can, at best, be reduced to a Jordan canonical form [16,22]. Since these matrices are extensively used for robotics and computer vision applications, Ghosal *et al.* [13] have tried to revolutionize these classical theories by demonstrating that these transformations can be diagonalized under a certain condition and the rule becomes the exception. In this work, we investigate the applicability of this technique for interpolating homogeneous bone rigid transformations and geometric transformations generated by a linear dynamical system. The diagonalizability of bone transformations under joint mechanical constraints is justified in section 2.2.2. Then, we employ this technique to propose a fast algorithm for evaluating a Log-Euclidean polyrigid transformations on a regular grid. The main advantage of our algorithm is its capacity to drastically reduce memory requirements.

To demonstrate the effectiveness of the proposed algorithm on both synthetic data and real dynamic MRI data, we performed an objective comparison between the two methods in terms of accuracy, computation time, and memory requirements. And we concluded that the eigendecomposition method is more capable of balancing the trade-off between them.

Finally, we have applied the eigendecomposition technique to estimate a smooth continuous curve of the ankle joint trajectory from a discrete set of bone transformations. This allowed to interpolate intermediate time frames in-between acquired time frames and thus to enhance the temporal resolution of the dynamic MRI sequence.

To resume, the main contributions of this work are:

- We define a trigonometric closed form for smooth parametrization of elements of $SE(3)$ without having to compute the matrix logarithms and exponentials in Section 2.2.1.
- We demonstrate the diagonalizability of human joint transformations in Section 2.2.2 and we propose to compute the exponential map using the eigendecomposition technique with fewer matrix multiplications in Section 2.2.3.
- We present an application of the proposed computational scheme in Section 3.2: spatio-temporal reconstruction of dynamic MRI sequences.

2 Methods

2.1 Smooth interpolation on $SE(3)$

2.1.1 Formulation of the interpolation problem

Consider two elements $T_a, T_b \in SE(3)$. The interpolation function to estimate a smooth trajectory between them according to a time-varying parameter $t \in [0, 1]$,

is given by:

$$\gamma : SE(3) \times SE(3) \times \mathbb{R} \rightarrow SE(3) \quad (1)$$

with:

$$\gamma(T_a, T_b, 0) = T_a \quad (2)$$

$$\gamma(T_a, T_b, 1) = T_b \quad (3)$$

The group element $T_c \in SE(3)$ that takes T_a to T_b can be obtained as follows:

$$T_c \equiv T_a^{-1} \circ T_b = T_b.T_a^{-1} \quad (4)$$

The function γ transforms the interpolation into the tangent space $se(3)$ for linearization purposes, and then transforms the resulting velocity vector back onto the manifold. A scaled map of T_c to the Lie Algebra $se(3)$ (where t is the scaling factor) is given by:

$$T_c(t) = t.log(T_c) \quad (5)$$

Finally, the exponential map allows for transforming back into the manifold, yielding the following interpolation function:

$$\gamma(T_a, T_b, t) = exp(T_c(t)).T_a \quad (6)$$

2.1.2 An ODE approach for the interpolation on $SE(3)$

Suppose now that we have the initial condition $T_a = id$, then the displacement of the rigid body can be modeled by the following autonomous first order ODE [6]:

$$\dot{\gamma}(t) = \gamma(t).log(T_b) \quad (7)$$

To simplify notations, we denote $T_b = T$. The solution of this ODE gives a smooth continuous curve of the rigid body trajectory (*i.e.* its optimal geodesic curve between two rigid body poses):

$$\gamma(t) = exp(t.log(T)) \quad for \quad t \in [0, 1] \quad (8)$$

The Equation (8) shows that the exponential map takes the linear tangential trajectory $t.log(T) \in se(3)$, into a one-parameter subgroup of $SE(3)$, satisfying $\gamma(t_1 + t_2) = \gamma(t_2).\gamma(t_1)$, for all t_1, t_2 . This gives a local parameterization for the geometric transformation T .

Based on Equations (4), (6), and (8), it is clear that the first formulation exhibits greater complexity than the ODE approach as it imposes additional matrix multiplications and inversion.

2.1.3 Smooth interpolation of polyrigid transformations

To move from simply rigid to polyrigid interpolation of geometric transformations, Arsigny et al. proposed a registration framework to deal with autonomous continuous-time dynamical systems [4]. The main idea is to parameterize a non-linear geometrical deformation with a small number of intuitive parameters by fusing a set of linear transformations into a global diffeomorphism, according to a predefined positive weighting functions.

Let $\mathcal{T} = \{T_i\}_{i \in \{1 \dots N\}}$ be a set of N transformations in $SE(3)$, then the associated Log-Euclidean Fréchet mean, representing the Riemannian equivalent of the Euclidean arithmetic mean, is obtained by minimizing the following metric dispersion:

$$f_m(T_1, \dots, T_N) = \underset{T}{\operatorname{argmin}} \sum_{i=1}^N w_i d^2(T, T_i) \quad (9)$$

where $d(\cdot, \cdot)$ is the distance associated to the Riemannian metric.

The resulting Log-Euclidean Fréchet mean is given by:

$$f_m(T_1, \dots, T_N) = \exp\left(\sum_{i=1}^N w_i \log(T_i)\right) \quad (10)$$

Finally, the polyrigid interpolation problem can be formulated as follows:

For a given point x in the source image D_{t_0} , the continuous-time trajectory of x from D_{t_0} to the target image D_{t_1} can be computed according to:

$$\Phi(\tilde{x}, t) = \exp\left(t \sum_{i=1}^N \tilde{w}_i(x) \log(T_i)\right) \cdot \tilde{x} \quad (11)$$

where $\tilde{x} = \begin{pmatrix} x \\ 1 \end{pmatrix}$; $\Phi(\tilde{x}, 0) = \tilde{x}$; $t \in [0, 1]$ is the time parameter; $T_i \in SE(3)$, is the rigid transformation of the component i from D_{t_0} to D_{t_1} ; N is the total number of rigid components; $\Phi(\cdot, t)$ is the infinitesimal diffeomorphism from source to target; \tilde{w}_i is a normalized weight function (i.e., $\sum_{i=1}^N \tilde{w}_i(x) = 1, \forall x \in D_{t_0}$) which defines the local influence of the i^{th} component displacement on the resulting transformation at x (see section 3.2.2).

2.1.4 Numerical computation of the exponential map

The matrix exponential of an $m \times m$ matrix T can be defined by the following convergent power series:

$$e^T = \sum_{n=0}^{\infty} \frac{T^n}{n!} = I_m + T + \frac{T^2}{2!} + \frac{T^3}{3!} + \dots \quad (12)$$

where I_m is the $m \times m$ identity matrix.

The computation of the exponential map for solving ODEs requires the development of a fast and efficient algorithm to deal with the repeated evaluation of the matrix exponential over a regular grid. In this context, Arsigny et al. have proposed a fast algorithm for the estimation of exponential map to parameterize

polyrigid transformations using the scaling and squaring method [3]. The scaling and squaring method [1, 17] is a recursive technique that exploits the fact that the matrix exponential can be easily estimated for matrices close to zero using the Padé approximants. This method is based on the relation $e^T = (e^{\frac{T}{2^s}})^{2^s}$. The scaling step consists of evaluating $e^{\frac{T}{2^s}}$ while the squaring step consists of squaring the approximant s times to finally obtain an estimation of e^T . The overall algorithm is composed of the three following steps:

- **Scaling step:** $T \leftarrow \frac{T}{2^s}$ so that $\|T\|_\infty \simeq 1$, and $\|T/2^s\| \leq 1/2$.
- **Padé approximant to e^T :** $r_m(T) = [m/m]$, with: $r_m(x) = p_m(x)/q_m(x)$;
 $p_m(x) = \sum_{i=1}^m \frac{(2m-i)!m!}{(2m)!(m-i)!} \frac{x^i}{i!}$; and $q_m(x) = p_m(-x)$, where m represents the degree of the Padé approximant. The resulting error satisfies:
 $e^x - r_m(x) = (-1)^m \frac{(m!)^2}{(2m)!(2m+1)!} x^{2m+1} + O(x^{2m+2})$.
- **Repeated squaring:** $e^T = (r_m(T))^{2^s}$.

In [3], the ODE integration is performed using the scaling and squaring method, based on the following equations:

$$\gamma(\cdot, t_j) = \left(\exp\left(\frac{1}{2^s} \sum_{i=1}^N \tilde{w}_i(\cdot) \log(T_i)\right) \right)^{t_j^{-1}} \quad (13)$$

$$\gamma(\cdot, 1) = \gamma(\cdot, \frac{1}{2^s}) \quad (14)$$

where $\gamma(\cdot, 0) = id$; s is called the scaling factor, and $t_j^{-1} \in \{1, 2 \dots 2^s\}$.

The efficiency of this technique over a regular grid is somehow comparable to that of the Fast Fourier Transform (FFT) according to Arsigny et al [3]. However, this method increases the computation time dramatically with an important increase of grid size because of the high memory requirements for storing all matrices in the main computer memory during the repeated squaring.

For example, if $s = 4$ in (14), 4 matrix multiplications are needed to compute the exponential map at each grid point, as follows:

$$\begin{aligned} \gamma(\cdot, \frac{2}{16}) &= \gamma(\cdot, \frac{1}{16}) \circ \gamma(\cdot, \frac{1}{16}), \\ \gamma(\cdot, \frac{4}{16}) &= \gamma(\cdot, \frac{2}{16}) \circ \gamma(\cdot, \frac{2}{16}), \\ \gamma(\cdot, \frac{8}{16}) &= \gamma(\cdot, \frac{4}{16}) \circ \gamma(\cdot, \frac{4}{16}), \end{aligned}$$

until we obtain:

$$\gamma(\cdot, 1) = \gamma(\cdot, \frac{8}{16}) \circ \gamma(\cdot, \frac{8}{16}).$$

In general, the total number of matrix multiplications required for obtaining the complete trajectory of the articulated system is given by $N_s = 2^s = \exp(s \cdot \log(2))$ so that the number N_s increases exponentially with the scaling factor. From another angle, the increase of the scaling factor has been recommended in [14] for enhancing the numerical accuracy of matrix exponentials and their inverses. A review of Higham's method is proposed later in [15] for assessing the same accuracy with fewer matrix multiplications by increasing the degree of the Padé approximant. In [3], Arsigny et al. recommended the use of a scaling factor $s \geq 6$ to obtain accurate and stable results.

2.2 Proposed approach

In this section, we define a closed form for smooth interpolation of simply rigid transformations, and then we investigate the diagonalizability of 4×4 homogeneous transformations and we propose to use a matrix diagonalization based method for fast computation of the exponential map with reduced memory consumption in the context of articulated registration.

2.2.1 Closed form expression for smooth interpolation on $SE(3)$ via the exponential map:

Let $T \in SE(3)$, then T has the form:

$$T = \begin{bmatrix} [R] & d \\ \mathbf{0} & 1 \end{bmatrix} \quad (15)$$

where $[R] \in SO(3)$ is a 3×3 rotation matrix; $\mathbf{0}$ is the 1×3 zero vector; and $d = (d_x, d_y, d_z)^T$ is a 3×1 translation vector.

Let θ_x, θ_y , and $\theta_z \in]-\pi, \pi]$ be the rotation angles performed by the rigid body about the x-axis, y-axis, and z-axis, respectively. Then for $\alpha_x = \text{atan2}(\sin(\theta_x), \cos(\theta_x))$; $\alpha_y = \text{atan2}(\sin(\theta_y), \cos(\theta_y))$; $\alpha_z = \text{atan2}(\sin(\theta_z), \cos(\theta_z))$; and $t \in [0, 1]$, we define the following closed form for smooth parameterization of T via the exponential map, without having to compute the matrix logarithm and exponential:

$$\mathbf{e}^{(t \cdot \log(\mathbf{T}))} = \begin{pmatrix} \cos(t \cdot \alpha_y) \cdot \cos(t \cdot \alpha_z) & -\cos(t \cdot \alpha_y) \cdot \sin(t \cdot \alpha_z) & \sin(t \cdot \alpha_y) & t \cdot d_x \\ \sin(t \cdot \alpha_x) \cdot \sin(t \cdot \alpha_y) \cdot \cos(t \cdot \alpha_z) + \cos(t \cdot \alpha_x) \cdot \sin(t \cdot \alpha_z) & -\sin(t \cdot \alpha_x) \cdot \sin(t \cdot \alpha_y) \cdot \sin(t \cdot \alpha_z) + \cos(t \cdot \alpha_x) \cdot \cos(t \cdot \alpha_z) & -\sin(t \cdot \alpha_x) \cdot \cos(t \cdot \alpha_y) & t \cdot d_y \\ -\cos(t \cdot \alpha_x) \cdot \sin(t \cdot \alpha_y) \cdot \cos(t \cdot \alpha_z) + \sin(t \cdot \alpha_x) \cdot \sin(t \cdot \alpha_z) & \cos(t \cdot \alpha_x) \cdot \sin(t \cdot \alpha_y) \cdot \sin(t \cdot \alpha_z) + \sin(t \cdot \alpha_x) \cdot \cos(t \cdot \alpha_z) & \cos(t \cdot \alpha_x) \cdot \cos(t \cdot \alpha_y) & t \cdot d_z \\ 0 & 0 & 0 & 1 \end{pmatrix}$$

proof:

Let R_x , R_y and R_z be the three rotation matrices performed by the rigid body, about each direction in the space, then we have:

$$R_x = \begin{bmatrix} 1 & 0 & 0 \\ 0 & \cos(\theta_x) & -\sin(\theta_x) \\ 0 & \sin(\theta_x) & \cos(\theta_x) \end{bmatrix} \quad (16)$$

$$R_y = \begin{bmatrix} \cos(\theta_y) & 0 & \sin(\theta_y) \\ 0 & 1 & 0 \\ -\sin(\theta_y) & 0 & \cos(\theta_y) \end{bmatrix} \quad (17)$$

$$R_z = \begin{bmatrix} \cos(\theta_z) & -\sin(\theta_z) & 0 \\ \sin(\theta_z) & \cos(\theta_z) & 0 \\ 0 & 0 & 1 \end{bmatrix} \quad (18)$$

For $(\theta_x, \theta_y, \theta_z) \in]-\pi, \pi]^3$, one can map each rotation matrix to its tangent space $so(3)$ using the trigonometric function $atan2$. This gives:

$$\log(R_x) = \begin{bmatrix} 0 & 0 & 0 \\ 0 & 0 & -\alpha_x \\ 0 & \alpha_x & 0 \end{bmatrix} \quad (19)$$

$$\log(R_y) = \begin{bmatrix} 0 & 0 & \alpha_y \\ 0 & 0 & 0 \\ -\alpha_y & 0 & 0 \end{bmatrix} \quad (20)$$

$$\log(R_z) = \begin{bmatrix} 0 & -\alpha_z & 0 \\ \alpha_z & 0 & 0 \\ 0 & 0 & 0 \end{bmatrix} \quad (21)$$

Then, we define the explicit forms for transforming back these transformations into the manifold $SO(3)$ as follows:

$$\exp(t.\log(R_x)) = \begin{bmatrix} 1 & 0 & 0 \\ 0 & \cos(t.\alpha_x) & -\sin(t.\alpha_x) \\ 0 & \sin(t.\alpha_x) & \cos(t.\alpha_x) \end{bmatrix} \quad (22)$$

$$\exp(t.\log(R_y)) = \begin{bmatrix} \cos(t.\alpha_y) & 0 & \sin(t.\alpha_y) \\ 0 & 1 & 0 \\ -\sin(t.\alpha_y) & 0 & \cos(t.\alpha_y) \end{bmatrix} \quad (23)$$

$$\exp(t.\log(R_z)) = \begin{bmatrix} \cos(t.\alpha_z) & -\sin(t.\alpha_z) & 0 \\ \sin(t.\alpha_z) & \cos(t.\alpha_z) & 0 \\ 0 & 0 & 1 \end{bmatrix} \quad (24)$$

Under the operation of composition, we obtain the exponential map associated to the rotation matrix $[R]$:

$$\exp(t.\log(R)) = \exp(t.\log(R_x)).\exp(t.\log(R_y)).\exp(t.\log(R_z)) \quad (25)$$

And finally, we obtain the desired result by simply scaling the translation vector:

$$\exp(t.\log(T)) = \begin{bmatrix} [\exp(t.\log(R))] & t.d \\ \mathbf{0} & 1 \end{bmatrix} \quad (26)$$

However, and as mentioned from the beginning, one cannot extend these closed forms to the parameterization of polyrigid transformations via the exponential map.

Proof:

The log Euclidean mean of N rigid transformations is given by:

$$\mathcal{T}(., t) = \exp \left(t \sum_{i=1}^N \tilde{w}_i(.) \log(T_i) \right) \quad (27)$$

We defined above a trigonometric closed form for smooth interpolation of each individual element of the special Euclidean group $SE(3)$. Since the elements of

$SE(3)$ are not necessarily commutative (*i.e.* $T_i.T_j \neq T_j.T_i$ for $i \neq j$ and $T_i, T_j \in SE(3)$), then the property $e^{(T_i+T_j)} = e^{T_i}.e^{T_j}$ is not verified and one cannot extend the proposed closed form to the polyrigid case.

2.2.2 Diagonalizability of the 4×4 homogeneous transformation matrices

Definition 1 Let T be a linear operator on the finite dimensional space V , then T is diagonalizable if there is a basis for V each vector of which is a characteristic vector (eigenvector) of T . One could also define T to be diagonalizable when the characteristic vectors of T span V .

In classical mechanics, one of the well known properties is that an homogeneous 4×4 transformation matrix cannot be diagonalized and can, at best, be reduced to a Jordan canonical form [22]. If we take the example of screw motion through the z - *axis*, the screw transformation will be:

$$T_\theta = \begin{bmatrix} \cos(\theta) & -\sin(\theta) & 0 & d_x \\ \sin(\theta) & \cos(\theta) & 0 & d_y \\ 0 & 0 & 1 & d_z \\ 0 & 0 & 0 & 1 \end{bmatrix} \quad (28)$$

where $T_\theta \in SE(3)$, $d = (d_x, d_y, d_z)$ is the translation vector, and θ is the rotation angle about the z - *axis*. In general, a rigid body displacement has a fixed line, called the screw axis. This axis is an invariant subspace of T_θ (*i.e.* it has the same spatial position before and after applying the transformation to the rigid body). Consider the eigenvalue problem $T_\theta v = \lambda v$, the associated characteristic equation is $\det(T_\theta - \lambda I_4) = (\lambda^2 - 2\lambda \cos(\theta) + 1)(1 - \lambda)^2 = 0$. Thus, the eigenvalues of T_θ in the complex domain are: $\{e^{i\theta}, e^{-i\theta}, 1, 1\}$. The pair of complex conjugate $\lambda_1 = e^{i\theta}$ and $\lambda_2 = \lambda_1^* = e^{-i\theta}$ are the eigenvalues of the rotational block and the corresponding eigenvectors $v_1 = (x_1, 0)$ and $v_2 = (x_2, 0) \in \mathbb{C}^4$ are four dimensional. Clearly, the eigenvectors associated with the repeated eigenvalue $\lambda_3 = \lambda_4 = 1$ satisfy $[T - I_4]v = 0$. By definition, the eigenvector v_3 associated to λ_3 is the one derived from the Euler-Rodrigues' vector b , $v_3 = (b, 0) = (\tan(\frac{\theta}{2}).s, 0)$ for $\theta \neq \{-\pi, \pi\}$, where s is the unit vector in along the screw axis. So that the eigenvectors corresponding to the double root $\lambda = 1$ are linearly dependant (*i.e.* the algebraic multiplicity of $\lambda = 1$ is two, different from its geometric multiplicity =1). Though T_θ does have a two dimensional invariant plane associated with this repeated eigenvalue. In that case, T_θ cannot be diagonalized and can, at best, be reduced to a Jordan canonical form.

In [13], Ghosal *et al.* proved that one can exclude non-pure-screw transformations from these assumptions. A screw transformation occurs when the motion consists of a rotation about a single axis with a non-zero displacement along the same axis. More specifically, a 4×4 homogeneous matrix with nontrivial rotation can be diagonalized if and only if the translation along the screw axis is zero (*e.g.* T_θ can be diagonalized if and only if the translation along the z - *axis*, $d_z = 0$). Under these constraints, Ghosal *et al.* demonstrated the existence and the non-uniqueness of a fourth eigenvector \tilde{v}_4 of the form $\tilde{v}_4 = (u, 0) + \epsilon(0, 0, 0, 1)$, linearly independent of $v_3 = (\tan(\frac{\theta}{2}).s, 0)$, and satisfying $[R - I_3]u = -\epsilon d$ where R is the 3×3 rotation submatrix of T and $\epsilon \neq 0$. As a consequence, the four distinct vectors $(x_1, 0), (x_2, 0), (b, 0)$, and (u, ϵ) form an eigenbasis of \mathbb{C}^4 and the matrix

T_θ is diagonalizable. If the displacement along the screw axis is non zero, Ghosal *et al.* presented a rigorous algebraic treatment proposing explicit expressions for the Jordan basis by means of a small perturbation of the original matrix near the screw axis.

In the context of articulated motion, the human bones may never be able to perform screw motions in normal conditions due to the natural joint mechanical constraints. This suggests that rigid bone transformations are always diagonalizable. Moreover, the entire joint complex (bones plus surrounding tissues) moves in harmony. This suggests that even the resulting joint polyrigid transformations must be diagonalizable as they cannot represent screw transformations. A numerical example is given in the Appendix 4.A.

2.2.3 Smooth interpolation of polyrigid transformations via matrix eigendecomposition

In the context of articulated registration, we propose to employ an eigenvalue-based method for smooth interpolation on $SE(3)$, assuming that the map from the Lie Algebra to the corresponding Lie group is performed according to the equation (8) for each of the bones.

Let $T \in SE(3)$ be the rigid transform to be interpolated, then there exist an invertible matrix P and a diagonal matrix D such that $T = PDP^{-1}$. The diagonal elements $\{\lambda_k\}_{k \in \{1 \dots 4\}}$ are the eigenvalues of T which satisfy the characteristic equation $\det(T - \lambda_k I_4) = 0$, while the columns of P are the corresponding eigenvectors $\{v_k\}_{k \in \{1 \dots 4\}}$ which satisfy the linear equation $Tv_k = \lambda_k v_k$, also known as the eigenvalue problem. Based on this matrix eigendecomposition, one can compute the rigid body trajectory with respect to (8) as follows:

$$\gamma(t) = P \cdot \text{diag}(e^{t \cdot \log(\lambda_1)}, e^{t \cdot \log(\lambda_2)}, e^{t \cdot \log(\lambda_3)}, 1) \cdot P^{-1} \quad (29)$$

Definition 2 A logarithm of $T \in \mathbb{C}^{n \times n}$ is any matrix X such that $e^X = T$.

The matrix logarithm of most practical interest is the one whose eigenvalues lie in the right half-plane, which is called the principal matrix logarithm. If T is nonsingular (*i.e.* if T is invertible) and has no eigenvalues on the negative real axis then T has a unique principal matrix logarithm. For a diagonalizable matrix T , $\log(T) = P \cdot \text{diag}(\log(\lambda_1), \log(\lambda_2), \log(\lambda_3), 0) \cdot P^{-1}$.

Thanks to the property $\exp(t \cdot \log(T)) = T^t$, one can reformulate the interpolation function as follows:

$$\gamma(t) = T^t = PD^t P^{-1} = P \cdot \text{diag}(\lambda_1^t, \lambda_2^t, \lambda_3^t, 1) \cdot P^{-1} \quad (30)$$

Changing t continuously from 0 to 1 will *infinitesimally* change the function $\gamma(t)$ from the *identity* to the matrix T . This allows for interpolating between two rigid body poses from an homogeneous geometric transformation, by directly scaling its eigenvalues where t is the scaling factor here. Figure 1 illustrates the linear interpolation of one simulated 3D rigid transformation using (30).

This technique can be also applied to interpolate any linear combination of bone rigid transformations and can thereby be embedded in the LEPF in this context.

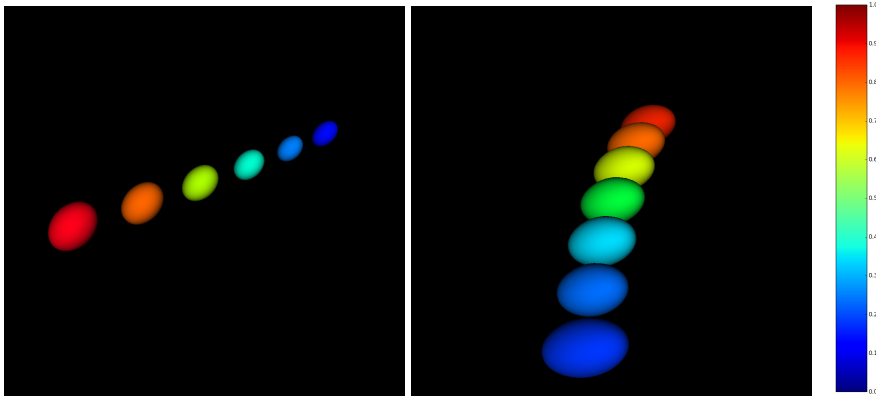


Fig. 1 Smooth interpolation of linear geometric transformations that map the blue ellipsoid (initial pose) to the red one (final pose), obtained by varying t from 0 to 1 in (30). From left to right: interpolation of a simulated affine transformation with the following parameters: translations: $(0, 0, 0mm)$, rotations: $(0, 0, 10^\circ)$, shearings: $(0, 0, 0)$, and scalings: $(1.5, 1.5, 1.5)$; interpolation of a simulated rigid transformation (a single rotation of 30° around the z -axis).

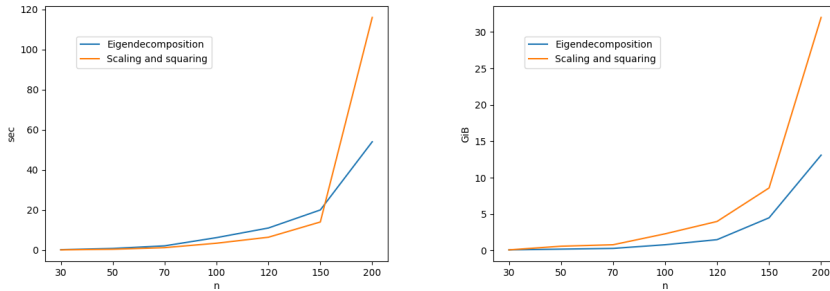


Fig. 2 Computation of the exponential map over an $n \times n \times n$ regular grid. From left to right: computation times, and memory requirements in function of the grid size.

3 Applications and results

3.1 Exponential map and parameterization of pure rotations: example of counterclockwise rotations

Let T_θ be the following 3×3 matrix,

$$T_\theta = \begin{bmatrix} a & -b & 0 \\ b & a & 0 \\ 0 & 0 & c \end{bmatrix},$$

letting $a = \cos(\theta)$; $b = \sin(\theta)$; and $c = 1$, then the matrix T_θ is the homogeneous rigid transformation which generates a counterclockwise rotation by θ

Table 1 Errors on exponential map estimates $\exp(\log(T_\theta))$ (ϵ_θ in the order of 10^{-16}). For the second method, the matrix logarithm is first approximated using an inverse scaling and squaring method [2] based on the fact that the principal matrix logarithm is much simpler to compute for matrices close to the *identity*.

Method	Error per rotation angle θ								
	$-\frac{\pi}{2}$	$-\frac{\pi}{4}$	$-\frac{\pi}{6}$	$\frac{\pi}{6}$	$\frac{\pi}{4}$	$\frac{\pi}{3}$	$\frac{\pi}{2}$	$\frac{2\pi}{3}$	$\frac{3\pi}{4}$
1. Eigendecomposition	3	2.4	2.3	2.3	2.4	2.4	3.2	2.5	1.2
2. Scaling and squaring	3.9	3.8	2.2	2.2	3.8	4.1	4.6	11	1.9

radians about the origin of a 2D cartesian coordinate system. The logarithm of the matrix T_θ , which maps T_θ to its tangent space, is unique for $-\pi < \theta < \pi$ rad and is equal to its *principal matrix logarithm*:

$$\log(T_\theta) = \begin{bmatrix} 0 & -\text{atan2}(b, a) & 0 \\ \text{atan2}(b, a) & 0 & 0 \\ 0 & 0 & 0 \end{bmatrix},$$

a one-parameter subgroup of the Lie group $SE(2)$, which is parametrized with the parameter t , is given by:

$$\exp(t \cdot \log(T_\theta)) = \begin{bmatrix} \cos(t \cdot \text{atan2}(b, a)) & -\sin(t \cdot \text{atan2}(b, a)) & 0 \\ \sin(t \cdot \text{atan2}(b, a)) & \cos(t \cdot \text{atan2}(b, a)) & 0 \\ 0 & 0 & 1 \end{bmatrix}.$$

For $t = 1$ and for different values of θ , Table 1 reports the error in the computation of the exponential map from the Lie algebra $se(2)$ to the corresponding Lie group $SE(2)$, using each of the two methods. This error is defined by: $\epsilon_\theta = \|\exp(\log(T_\theta)) - T_\theta\|_2$.

Table 1 shows that both methods are prone to neglectable rounding errors: occurring during the matrix inversion and multiplications for the eigendecomposition method; and during the repeated squarings for the scaling and squaring method. This confirms that both methods have nearly the same precision.

In order to compare the performances of the two methods in terms of computation times, we have generated a set of regular grids with a size of $(n \times n \times n \times 4 \times 4)$, with $n \in \{30, 50, 70, 100, 120, 150, 200\}$. Each element of each grid is equal to $V = \log(T_{\frac{\pi}{4}})$, where $T_{\frac{\pi}{4}}$ is the homogeneous rigid transformation $\in SE(3)$ that encodes a counterclockwise rotation by $\frac{\pi}{4}$ radians around the z -axis. Our code is implemented in *Python* using the LAPACK (Linear Algebra Package) routines for computing the exponential map: we have used the routine *tensorflow.linalg.expm* which uses a combination of the scaling and squaring method and the Padé approximation (this routine optimizes the scaling factor automatically in order to increase the computational accuracy, depending on the matrix norm; for example for matrices *very close* to zero, the minimal possible scaling factor 2 is used), and the routine *numpy.linalg.eig* to compute the matrix eigenvalues and eigenvectors. All experiments are performed on an Intel[®] Xeon[®] Processor E3-1271 v3 3.60 GHz, with a physical memory of 32GB.

Both methods are fast and numerically stable for sparse regular grids (*i.e.*, for $n \leq 100$). As illustrated in Figure 2, the eigendecomposition method is twice slower than the scaling and squaring method for sparse grids because of the additional time required for matrix inversion and multiplications, after solving the *eigenvalue problem*. However, the scaling and squaring method increased the computation time dramatically with an important increase of grid size (*i.e.*, for $n = 200$) because of the high memory requirements for storing all matrices in the main computer memory during the repeated squarings.

3.2 Application to the enhancement of temporal resolution of dynamic MRI sequences

3.2.1 Motivation

Dynamic MRI is a *non-invasive* imaging technique that allows to qualitatively assess the behavior of the human joints *in vivo*. Real-time Fast Field Echo (FFE) sequences have the potential to reduce the effect of motion artifacts by acquiring the image data within a few milliseconds [26]. However, the short acquisition times affect the temporal resolution of the acquired sequences (*i.e.* the scanning duration is short relative to the joint motion). In this work, we propose to reconstruct the missing frames of the sequence given the reduced amount of acquired data, by applying the proposed motion interpolation technique which is based on scaling the transformation eigenvalues. This leads to estimate a continuous-time trajectory of the joint from a discrete set of rigid-body poses. To do this: we first estimate the rigid motion of each bone from the acquired discrete data using a robust intensity-based registration algorithm. Then, we fuse these local transformations into a global diffeomorphisms to compute the non-linear joint deformations between successive images according to (11). The idea is to reconstruct the missing time frames by interpolating the joint velocity vector field and then transforming the resulting *infinitesimal* velocity vector field back onto the manifold via the exponential map. The algorithm has been applied and validated using dynamic data from five subjects performing passive ankle dorsi-plantar flexion.

3.2.2 Estimation of temporal joint deformation field

The joint deformation field between each successive acquired time frames is estimated by fusing a set of rigid body transformations $\{T_i^{t_j}\}_{i \in 1 \dots N}^{j \in 1 \dots L-1}$ (corresponding to the bones of interest, where L is the length of the acquired discrete sequence), according to Eq (11). A continuous trajectory of the joint is then obtained by varying the time parameter from 0 to 1.

In [8,9], *Commowick et al.* proposed an inverse-distance based weighting function that preserves bone shapes after registration (31). However, such weighting functions yield inaccurate deformation outside the segmented bones.

$$w_i^{t_j}(x) = \frac{1}{1 + \alpha \cdot \text{dist}(x, B_i^{t_j})^\beta} \quad (31)$$

where $x \in D^{t_j}$, $B_i^{t_j}$ is the binary mask of the i^{th} component, and $\text{dist}(\cdot, B_i^{t_j})$ is the corresponding Euclidean distance map at time t_j (see Figure 3).

As illustrated in Figure 7, experiments show that an increase in β in Eq (31) increases the accuracy of the estimated deformation field. Inspired by the relation ($e^x \gg x^\beta$, when $x \rightarrow +\infty$), we have redefined the associated weight functions $\{w_i^{t_j}\}_{i \in 1 \dots N}$ as follows [21]:

$$w_i^{t_j}(x) = \frac{2}{1 + \exp(\gamma \cdot \text{dist}(x, B_i^{t_j}))} \quad (32)$$

To take into account the effects of all dependee components during fusion, each component weight function is normalized as follows:

$$\tilde{w}_i^{t_j} = \frac{w_i^{t_j}}{\sum_{i=1}^N w_i^{t_j}} \quad (33)$$

Figure 4 illustrates each bone normalized weight function as defined in (32). Finally, the source image intensities are mapped to new coordinates in the target image space by spline interpolation. The robustness of the method and the accuracy of the results have been evaluated using a local leave-one-out cross-validation technique. All results on joint motion estimation and interpolation are validated and reported in [21].

The exponential map of Eq (11) is computed within 2.2 seconds on a $352 \times 352 \times 6$ grid using the scaling and squaring method (which required 1.8 GB of RAM), and within nearly 4 seconds using the proposed eigendecomposition method (which required 0.8 GB of RAM). Figure 5 illustrates the interpolation quality of one 3D+time MRI sequence from our dataset.

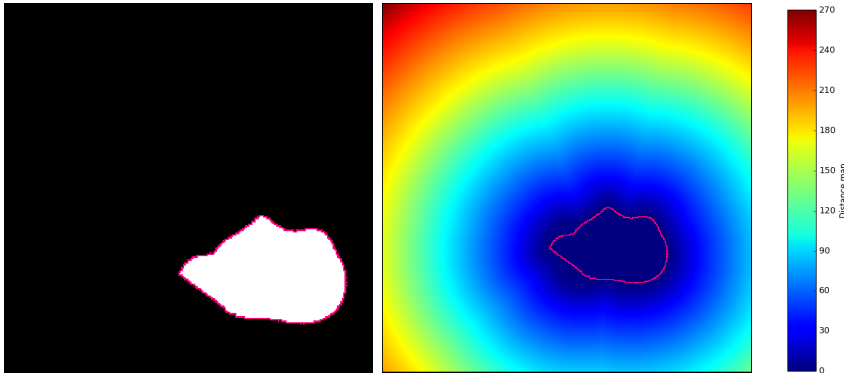


Fig. 3 Euclidean distance map, from left to right: binary mask of the calcaneus; associated 3D Euclidean distance map.

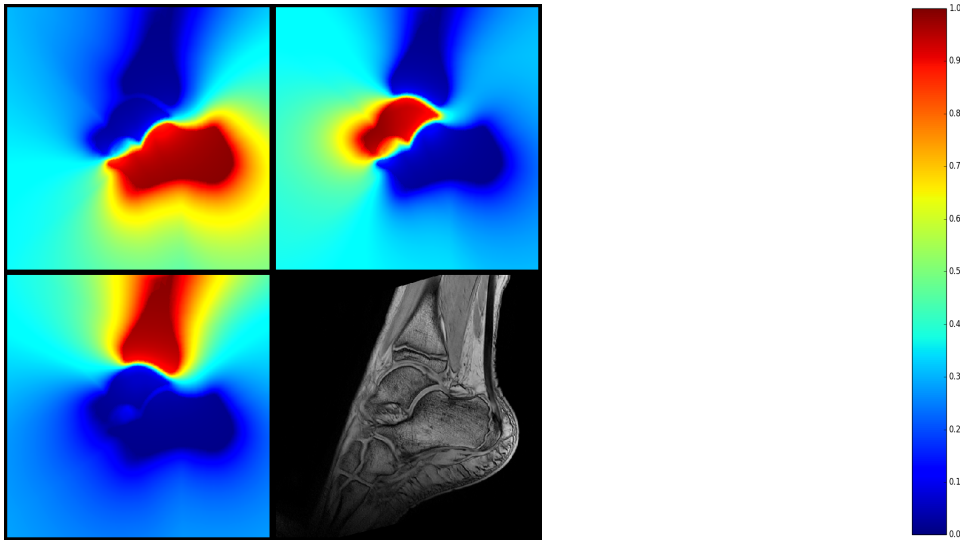


Fig. 4 Normalized weighting functions: from up to down, from left to right: for the calcaneus; for the talus; for the tibia; and the associated MRI scan.

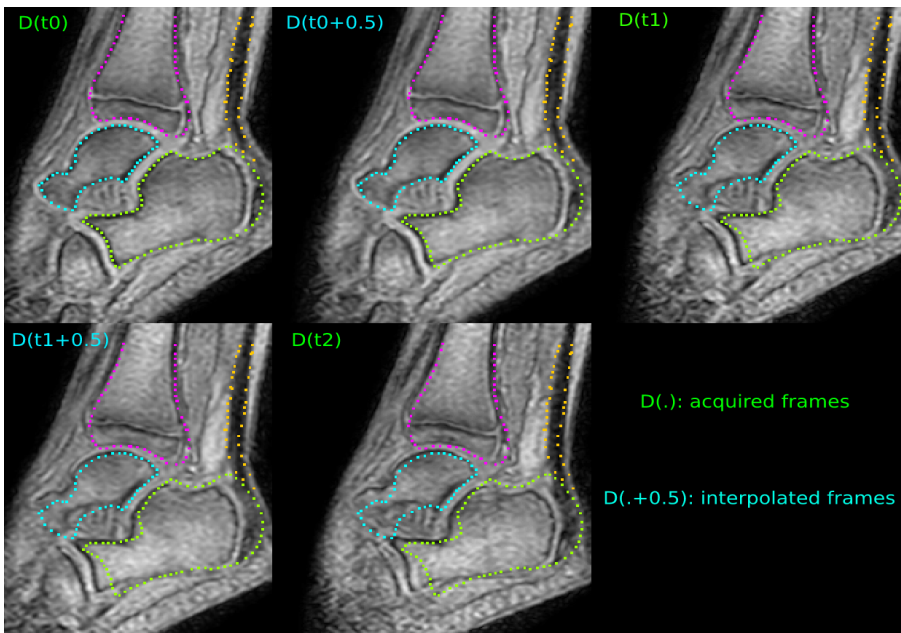


Fig. 5 Interpolation of missing time frames using the proposed eigendecomposition method: $D(t_j)$ is the j^{th} acquired time frame; while $D(t_j + 0.5)$ is the time frame half way between $D(t_j)$ and $D(t_{j+1})$ (i.e., $t = 0.5$ in (11)), for $j \in \{0, 1, 2\}$. Bone contours have been drawn in the first time frame to show the interpolation quality and the relative joint motion.

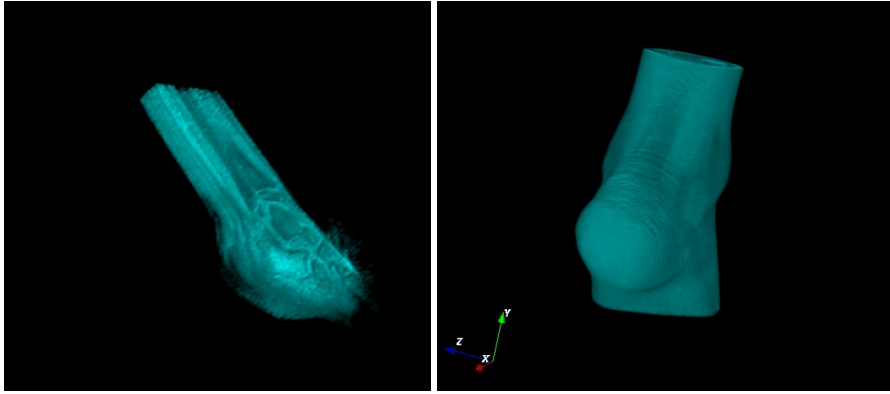


Fig. 6 High-resolution reconstruction of dynamic time frames. From left to right: the first low resolution acquired frame; and the corresponding volume, reconstructed in the same resolution of the static MRI scan.

3.3 Discussion

If m is the total number of intermediate points chosen to discretize the continuous trajectory of each point x , the scaling and squaring method is the most commonly used technique for computing the matrix exponential in previous works [3, 9, 12, 25]. However, the use of this method results in excessive memory requirements as it requires multiple matrix multiplications (see Figure 2) and thus it is not suitable for estimating or interpolating very dense deformation fields (*e.g.* when registering very high-resolution MRI data [19]). To overcome this limitation, we have proposed to compute the matrix exponential using matrix eigendecomposition. The grid is interpreted as a tensor of $dim_0 \times dim_1 \times dim_2$ matrices, each of size 4×4 (with dim_0 , dim_1 , and dim_2 are the image dimensions), and the trajectories of all the points of the regular grid are computed simultaneously. Furthermore, computations are performed in the complex domain: for all real transformation matrices expressed in homogeneous coordinates, the associated eigenvalues occur in complex-conjugate pairs where the imaginary part of the eigenvalue is the frequency of voxel rotation.

Both methods lead to nearly the same level of accuracy and they can also reach the machine precision since the error is always of order 10^{-16} .

For sparse regular grids, the eigendecomposition method is a little slower than the scaling and squaring method, but it offers much faster computations in the case of dense regular grids. Hence, this method is more capable of balancing the trade-off between computation times and memory requirements. For example, the optimization of large storage requirements could be very useful when estimating a dense deformation field from a high-resolution static MRI scan to a low-resolution dynamic time frame [19, 20]. In these previous works, a deformation vector field of $576 \times 576 \times 202 \approx 67$ millions deformation vectors is computed in 15 min using the eigendecomposition method while consuming the entire physical memory (32GB). However, the use of the scaling and squaring method for estimating the same deformation vector field results severe memory swapping which drastically slows down computations until totally stopping the computation process. Figure 6

illustrates the high resolution reconstruction of the ankle joint by estimating a dense deformation field from the static scan to a low-resolution time frame from the MRI sequence.

The eigendecomposition method allows for interpolating the desirable number of intermediate points and thus for obtaining a smooth and continuous trajectory of the dynamical system by scaling the transformation eigenvalues, without the need to perform a large number of matrix multiplications. In fact, once the *eigenvalue problem* is solved over the regular grid, the transformation eigenvalues and the sub-matrices containing the associated eigenvectors (with their inverses) can be stored in the main computer memory, and the interpolation of an intermediate point requires only two matrix multiplications.

The proposed interpolation technique can be also extended to diagonalizable *polyaffine* transformations, for which local transformations to be fused offers additional degrees of freedom like the scalings and shearings. Figure 1 illustrates the consistent interpolation of a simulated affine transformation using matrix eigendecomposition.

In most applications such as human skeleton tracking during motion, the amount of local rotation of each rigid component is strictly below π radians, so that the matrix logarithm of a bone transformation T exists always and is equal to the *principal matrix logarithm*. This suggests that the property $\exp(t.\log(T)) = T^t$, is verified for these transformations. Concerning the diagonalizability of 4×4 homogeneous rigid transformations, we argue that the joint bones may never be able to perform screw motions in normal conditions due to the effect of mechanical constraints on the joint motion. Hence, the estimated bone transformations expressed in homogeneous coordinates possess 4 linearly independent eigenvectors and thus are always *diagonalizable*.

In this work, a motion-interpolation-based method for increasing the temporal resolution of anatomical dynamic MRI sequences is presented. We have generalized the LEPF to dynamic articulated structures and we have also proposed new weight functions to increase the local effect of bone transformations on the deformations of the surrounding tissues. The proposed inverse-distance-based weight functions are more suitable than the Gaussian weight functions [27] for articulated registration. Since the Gaussian weight functions induces some smoothing which affects the bone shapes by affecting sharp peaks particularly. Both our new weight functions and the weight functions defined in [8,9] conserve the bone topologies. However, our weight functions yield more accurate deformation vectors outside the skeleton as illustrated in Figure 7 for the Achilles tendon deformations.

The proposed post processing pipeline aims to overcome the physical limitations related to real-time dynamic MR imaging algorithms which are generally based on compressed sensing theory [18], for which it is hard to fastly acquire the entire or nearly the entire joint trajectory inside the MR scanner because of the limited k -space sampling.

4 Conclusion

In this paper, we proposed a fast and efficient algorithm to compute the exponential map for solving ODEs modeling the evolution of dynamical systems over

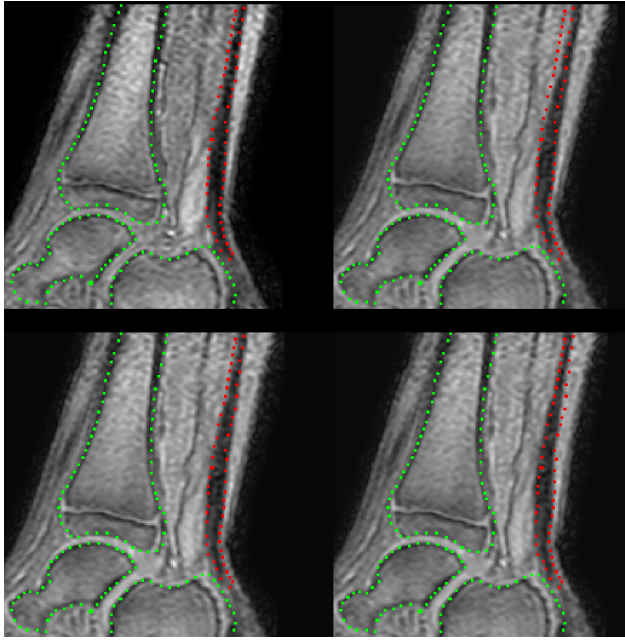


Fig. 7 Effects of different weight functions to the estimation of deformation fields. From left to right, from up to down: target image; image reconstructed using (31) with $\alpha = 0.5$ and $\beta = 1$; image reconstructed using (31) with $\alpha = 0.5$ and $\beta = 2$; image reconstructed using eq (32) with $\gamma = 0.1$. All contour points are drawn in the target image.

a regular grid. An objective comparison between the eigendecomposition method and the scaling and squaring technique used in previous studies is performed using simulated data and four dimensional (3D + time) dynamic MRI data. Experiments show that the scaling and squaring method is more suitable for sparse grids since computational burden and memory requirements grow exponentially with grid size. The obtained results demonstrate also the potential of the eigendecomposition method to optimally balance the trade-off between accuracies, computation times, and memory requirements for the computation of the exponential map.

Acknowledgements This work was supported by the French region of Brittany and the chaire d'excellence INSERM, IMT Atlantique. The authors wish to express their thanks to prof. Nicholas J.Higham for feedback and for valuable comments about this work.

* The source code is available on github: https://github.com/rousseau/dynMRI/blob/master/Exponential_map.py

4.A Appendix: numerical example:

In this appendix, we provide a numerical example of the computation of eigenvalues and eigenvectors of realistic bone rigid transforms. Let T_0 , T_1 and T_2 be the estimated rigid transformations between two successive acquired time frames, for calcaneus, talus, and tibia, respectively.

Table 2 experimental results.

Matrix	Rotations(deg)	Translations(mm)	λ_3
T_0	(-0.802, 1.203, -6.087)	(-10.09, 11.21, 3.38)	$1.00030947 + 0.i$
T_1	(1.777, 1.261, -4.302)	(-7.6, 8.603, 0.174)	$0.99982089 + 0.i$
T_2	(-0.172, -0.286, 0.114)	(-0.551, 0.1245, 0.092)	$1 + 0.i$

$$T_0 = \begin{bmatrix} 0.9941718578 & 0.1057560965 & 0.02092652582 & -10.089325 \\ -0.1060616449 & 0.9942600131 & 0.01407066546 & 11.20823699 \\ -0.0193183478 & -0.01620816253 & 0.9996820092 & 3.384391194 \\ 0 & 0 & 0 & 1 \end{bmatrix} \quad (34)$$

$$T_1 = \begin{bmatrix} 0.9969449639 & 0.07495416701 & 0.02196962386 & -7.610509439 \\ -0.0742572844 & 0.9967576861 & -0.03098434582 & 8.603319055 \\ -0.02422079816 & 0.02925828099 & 0.9992784262 & 0.1743830604 \\ 0 & 0 & 0 & 1 \end{bmatrix} \quad (35)$$

$$T_2 = \begin{bmatrix} 0.9999853969 & -0.002367701847 & -0.004865686409 & -0.5515243692 \\ 0.002382844221 & 0.9999923706 & 0.003108616918 & 0.1245495693 \\ 0.004858288914 & -0.003120165784 & 0.9999833703 & 0.09221866638 \\ 0 & 0 & 0 & 1 \end{bmatrix} \quad (36)$$

From Table 2, it is clear that T_0 and T_1 possess four distinct eigenvalues since $\lambda_1 = \lambda_2^*$ and $\lambda_3 \neq \lambda_4 = 1$. However, T_2 has a repeated eigenvalue $\lambda_3 = \lambda_4 = 1$ (which was expected since T_2 is very close to the identity so that all its eigenvalues should be equal or nearly equal to 1). All bones typically rotate about the three axes to maintain joint stability. For example, the tibial motion is not a pure screw motion and the matrix T_2 can be diagonalized as demonstrated in Section 2.2.2, and it has the following eigenvectors:

$$\begin{aligned} v_1 &= (0.12 + i0.6; \quad 0.197 - i0.36; \quad 0.67; \quad 0), \\ v_2 &= (0.12 - i0.6; \quad 0.197 + i0.36; \quad 0.67; \quad 0), \\ v_3 &= (-0.49; \quad -0.81; \quad 0.32; \quad 0), \end{aligned}$$

and,

$$\tilde{v}_4 = (0.49; \quad 0.81; \quad -0.32; \quad \epsilon = 1.13 * 10^{-15}).$$

Then, v_1, v_2, v_3 , and \tilde{v}_4 form an eigenbasis of \mathbb{C}^4 and T_2 is also diagonalizable despite the fact that it has a repeated eigenvalue.

Table 2 illustrates the fact that each bones rotates simultaneously about the three axes, which confirms our hypothesis suggesting that the human bones may never be able to perform pure screw transformations under the joint mechanical constraints.

Let now $V = a \log(T_0) + b \log(T_1) + c \log(T_2)$ be a velocity. Then for: $a = 0.3, b = 0.2$, and $c = 0.5$, the complex eigenvalues of V are $\{\lambda_1 = -2, 9.10^{-5} - i \ 4, 6.10^{-2}; \lambda_2 = -2, 9.10^{-5} + i \ 4, 6.10^{-2}; \lambda_3 = 4, 6.10^{-5} - i \ 7, 5.10^{-28}; \lambda_4 = 0\}$. These eigenvalues are distincts and consequently V is diagonalizable.

References

1. Al-Mohy, A.H., Higham, N.J.: A new scaling and squaring algorithm for the matrix exponential. *SIAM Journal on Matrix Analysis and Applications* **31**(3), 970–989 (2009)
2. Al-Mohy, A.H., Higham, N.J.: Improved inverse scaling and squaring algorithms for the matrix logarithm. *SIAM Journal on Scientific Computing* **34**(4), C153–C169 (2012)
3. Arsigny, V., Commowick, O., Ayache, N., Pennec, X.: A fast and log-euclidean polyaffine framework for locally linear registration. *Journal of Mathematical Imaging and Vision* **33**(2), 222–238 (2009)
4. Arsigny, V., Commowick, O., Pennec, X., Ayache, N.: A log-euclidean polyaffine framework for locally rigid or affine registration. In: *International Workshop on Biomedical Image Registration*, pp. 120–127. Springer (2006)
5. Arsigny, V., Fillard, P., Pennec, X., Ayache, N.: Geometric means in a novel vector space structure on symmetric positive-definite matrices. *SIAM journal on matrix analysis and applications* **29**(1), 328–347 (2007)
6. Belta, C., Kumar, V.: New metrics for trajectory generation and interpolation on $SE(3)$
7. Belta, C., Kumar, V.: On the computation of rigid body motion. *Electron. J. Comput. Kinematics* **1** (2002)
8. Commowick, O., Arsigny, V., Costa, J., Ayache, N., Malandain, G.: An efficient locally affine framework for the registration of anatomical structures. In: *3rd IEEE International Symposium on Biomedical Imaging (ISBI 2006)*, pp. 478–481. IEEE (2006)
9. Commowick, O., Arsigny, V., Isambert, A., Costa, J., Dhermain, F., Bidault, F., Bondiau, P.Y., Ayache, N., Malandain, G.: An efficient locally affine framework for the smooth registration of anatomical structures. *Medical Image Analysis* **12**(4), 427–441 (2008)
10. Crum, W.R., Hartkens, T., Hill, D.: Non-rigid image registration: theory and practice. *The British journal of radiology* **77**(suppl_2), S140–S153 (2004)
11. Durrleman, S., Prastawa, M., Charon, N., Korenberg, J.R., Joshi, S., Gerig, G., Trounev, A.: Morphometry of anatomical shape complexes with dense deformations and sparse parameters. *NeuroImage* **101**, 35–49 (2014)
12. Ehrhardt, J., Ahlborg, M., Uzunova, H., Buzug, T.M., Handels, H.: Temporal polyrigid registration for patch-based mpi reconstruction of moving objects. *International Journal on Magnetic Particle Imaging* **4**(2) (2019)
13. Ghosal, A., et al.: A note on the diagonalizability and the jordan form of the 4×4 homogeneous transformation matrix. *Journal of Mechanical Design* **128**(6), 1343–1348 (2006)
14. Higham, N.J.: The scaling and squaring method for the matrix exponential revisited. *SIAM Journal on Matrix Analysis and Applications* **26**(4), 1179–1193 (2005)
15. Higham, N.J.: The scaling and squaring method for the matrix exponential revisited. *SIAM review* **51**(4), 747–764 (2009)
16. Hoffman K, K.R.: *Linear Algebra* (2nd Edition). Prentice Hall (1971)
17. Li, C., Zhu, X., Gu, C.: Matrix padé-type method for computing the matrix exponential. *Applied Mathematics* **2**(02), 247 (2011)
18. Lustig, M., Donoho, D.L., Santos, J.M., Pauly, J.M.: Compressed sensing MRI. *IEEE signal processing magazine* **25**(2), 72 (2008)
19. Makki, K., Borotikar, B., Garetier, M., Brochard, S., Salem, D.B., Rousseau, F.: High-resolution temporal reconstruction of ankle joint from dynamic MRI. In: *2018 IEEE 15th International Symposium on Biomedical Imaging (ISBI 2018)*, pp. 1297–1300. IEEE (2018)
20. Makki, K., Borotikar, B., Garetier, M., Brochard, S., Salem, D.B., Rousseau, F.: In vivo ankle joint kinematics from dynamic magnetic resonance imaging using a registration-based framework. *Journal of biomechanics* **86**, 193–203 (2019)
21. Makki, K., Borotikar, B., Garetier, M., Brochard, S., Salem, D.B., Rousseau, F.: Temporal resolution enhancement of dynamic mri sequences within a motion-based framework. In: *2019 IEEE 41st International Engineering in Medicine and Biology Conference (EMBC 2019)*. IEEE (2019)
22. McCarthy, J.M.: *Introduction to theoretical kinematics*. MIT press (1990)
23. Moler, C., Van Loan, C.: Nineteen dubious ways to compute the exponential of a matrix. *SIAM review* **20**(4), 801–836 (1978)
24. Moler, C., Van Loan, C.: Nineteen dubious ways to compute the exponential of a matrix, twenty-five years later. *SIAM review* **45**(1), 3–49 (2003)
25. Porras, A.R., Paniagua, B., Ensel, S., Keating, R., Rogers, G.F., Enquobahrie, A., Linguraru, M.G.: Locally affine diffeomorphic surface registration and its application to surgical planning of fronto-orbital advancement. *IEEE transactions on medical imaging* **37**(7), 1690–1700 (2018)

-
26. Schaeffter, T., Weiss, S., Eggers, H., Rasche, V.: Projection reconstruction balanced fast field echo for interactive real-time cardiac imaging. *Magnetic Resonance in Medicine: An Official Journal of the International Society for Magnetic Resonance in Medicine* **46**(6), 1238–1241 (2001)
 27. Seiler, C., Pennec, X., Reyes, M.: Capturing the multiscale anatomical shape variability with polyaffine transformation trees. *Medical Image Analysis* **16**(7), 1371–1384 (2012)
 28. Vemulapalli, R., Arrate, F., Chellappa, R.: Human action recognition by representing 3D skeletons as points in a lie group. In: *Proceedings of the IEEE conference on computer vision and pattern recognition*, pp. 588–595 (2014)
 29. Yu, H., Zhou, X., Jiang, H., Kang, H., Wang, Z., Hara, T., Fujita, H.: Learning 3D non-rigid deformation based on an unsupervised deep learning for pet/ct image registration. In: *Medical Imaging 2019: Biomedical Applications in Molecular, Structural, and Functional Imaging*, vol. 10953, p. 109531X. International Society for Optics and Photonics (2019)
 30. Žefran, M., Kumar, V.: Interpolation schemes for rigid body motions. *Computer-Aided Design* **30**(3), 179–189 (1998)